ABSTRACT

Title of Thesis: MEASURING THE EFFECT OF A PRESCRIBED BURN ON NITRIFICATION-COUPLED DENITRIFICATION IN A RESTORED CHESAPEAKE BAY TIDAL MARSH

Julia Catherine Charest, Master of Science, 2025

Thesis Directed By: Associate Research Professor Lorie Staver, Marine, Estuarine, and Environmental Science

Prescribed burning is a management practice used in tidal marshes of the Mid-Atlantic United States to improve habitat for wildlife. The impact of burning on tidal marsh biogeochemical processes, especially coupled nitrification-denitrification, has not been characterized. This study investigated the effect of burning on nitrification coupled denitrification in a restored tidal marsh on Poplar Island, Maryland, United States. A prescribed burn was completed in March 2024 to remove overwintering habitat for stem-boring insects. Soil-water exchange of gases and nutrients and soil pore water nutrients were measured before and after the prescribed burn. A nitrate addition experiment was conducted to explore the importance of dissimilatory nitrate reduction to ammonium. Soil-water exchange did not respond to burning, though strong interannual variation in denitrification was detected, with high rates measured in July 2023. The nitrate addition experiment revealed an increase in ammonium production, indicating the presence of the DNRA pathway in Poplar's marshes.

# MEASURING THE EFFECT OF A PRESCRIBED BURN ON NITRIFICATION-COUPLED DENITRIFICATION IN A RESTORED CHESAPEAKE BAY TIDAL MARSH

by

Julia Catherine Charest

Thesis submitted to the Faculty of the Graduate School of the
University of Maryland, College Park, in partial fulfillment
of the requirements for the degree of
Master of Science
2025

Advisory Committee:

Associate Research Professor Lorie Staver, Chair

Research Professor Jeffrey Cornwell

Associate Professor Jacob Cram

# Dedication

This thesis is dedicated to my parents, who have always been my biggest cheerleaders. Thanks Mom and Dad for all your love and support, and for always encouraging me to pursue my passions.

# Acknowledgements

I would like to thank my graduate committee; Drs. Lorie Staver, Jeff Cornwell, and Jacob Cram for their expertise, guidance, support, and encouragement over the last two and a half years. Each in their own way has helped me develop as a researcher and shown me confidence in my work and myself that I didn't even know I had. Thanks to Mike Owens, for his scientific expertise and guidance, as well as countless hours in the field and lab. His patience and understanding were much appreciated as I developed my understanding of these laboratory techniques under his guidance. Thanks to those who braved marsh-walking and summer heat with me to collect data including Amanda Schwark, Emily Coleman, Ben Malmgren, Kerry Burns, Gabi Chen, Summer Walker, and Kaelyn Gurka. I especially want to thank my lab mates Amanda and Emily for being able to laugh through challenges in the field and for making these last two years so fun.

I would like to acknowledge Maryland Environmental Service (MES) and the Maryland Port Administration for financial support for this research. Thank you to Claire Ruark, Mary Grace Antioch, and others at MES for their continuous logistical support and assistance. I would also like to acknowledge Horn Point Laboratory Education Committee for travel funding to share this work at the 14$^{th}$ International Symposium on Biogeochemistry of Wetlands and Aquatic Systems.

Finally, I would like to thank my family and friends, both here in Maryland and back in the Northeast, for supporting me in my graduate studies, especially those of you who travelled across several states to visit the Eastern Shore of Maryland. Thank you to my community in Maryland for making it feel like a home away from home.

# Table of Contents

# List of Figures

# Chapter 1

## *Introduction*

Tidal marshes provide valuable ecosystem services to coastal communities, including flood and erosion control, improvement of water quality, and important habitat for birds, commercial fish, and shellfish (Barbier et al., 2011). Tidal marshes are found around the world, mainly in temperate zones. Locally, Chesapeake Bay is home to 282,291 acres of tidal wetlands (Chesapeake Bay Program, https://www.chesapeakebay.net/issues/whats-at-risk/wetlands#:~:text=Shrub%20wetlands%2C%20known%20as%20bogs,runoff%20and%20weakening%20storm%20surges). These important Bay ecosystems are vulnerable to losses due to development, invasive species, and sea level rise. Restoration efforts around the Bay have established new wetlands where they did not previously exist, re-established or rehabilitated degraded wetlands, and enhanced wetlands to benefit wildlife (Chesapeake Bay Program, https://www.chesapeakebay.net/issues/whats-at-risk/wetlands#:~:text=Shrub%20wetlands%2C%20known%20as%20bogs,runoff%20and%20weakening%20storm%20surges). One such restoration project, the Paul S. Sarbanes Ecosystem Restoration Project at Poplar Island (Poplar Island), located in the mid-Bay region in Talbot County, focuses on the re-establishment of the island through the beneficial use of dredge materials from navigation channels approaching Baltimore Harbor.

Upon completion, Poplar Island will have about 314 hectares of wetland habitat (Staver et al., 2021). The dredge materials used in this project are nutrient-rich (Cornwell et al., 2020), leading to robust growth of species like *Spartina alterniflora* at low marsh elevations. However, enrichment of nutrients can also have negative consequences for marsh vegetation, potentially

including marsh dieback. Dieback has been documented in most of Poplar Island's marshes (Staver et al., 2020). One potential explanation is that P-rich soils have made the plants less resistant to pathogens and herbivores due to high growth rates of young tissue that possess decreased defenses, and greater palatability caused by increased production of amino acids (Marschner, 2012). One class of herbivores of interest are stem-boring insects, whose larvae are found in the stems of *S. alterniflora* on Poplar Island. Stem borers cause physical damage to plants by consuming tissue involved in transportation of water and nutrients, and wounds caused by insects can become infected by pathogens (Sobek and Munkvold, 1999).

While natural marshes lose standing dead plant material to outgoing tides, the dikes surrounding the Poplar Island marshes limit export (Staver et al., 2020). This leaves an optimal habitat for stem-boring insects to overwinter. This work expands on a study investigating the hypothesis that prescribed burning can mitigate marsh dieback by reducing overwintering habitat for stem-borers and pathogens, therefore promoting marsh vegetation health. The potential for unintended consequences to ecosystem functioning, such as alteration of nutrient cycles, remains unaddressed. In most marshes, burning likely does not affect denitrification rates, as they are usually limited by nitrate availability (Nyman and Chabreck, 1995). To address any potential consequences, this study explored the effect of the prescribed burn on Poplar Island on the coupled nitrification and denitrification reactions in the marsh soils.

Denitrification is the reduction of nitrate ($NO_3^-$) derived from overlying water or microbial nitrification (Equation 1) to nitrogen gas ($N_2$, Equation 2), which is returned to the atmosphere. It is an anaerobic reaction, used by microorganisms as an alternative to aerobic respiration in anoxic wetland soils (Schlesinger and Bernhardt, 2013). This process is particularly important in ecosystems where increased agriculture and other human activity have

created an excess of inorganic nitrogen in ambient waters (Verhoeven, 2006). For example, nutrients from fertilizers used by farmers and municipal and residential wastewater in the Chesapeake Bay watershed are carried by runoff through rivers and tributaries into the Bay. From 1945 to 1990, Susquehanna River nitrogen concentrations increased 2.5-fold (Kemp et al., 2005). This nutrient loading can be detrimental to the Bay's ecosystem. Eutrophication is responsible for harmful algal blooms, oxygen depletion in bottom waters, and loss of submerged aquatic vegetation (Fisher et al., 2006). Wetlands can remove excess N via burial and denitrification and prevent it from reaching the estuary (Verhoeven, 2006).

**Equation 1.** $2NH_3 + 3O_2 \rightarrow 2NO_2 + 2H^+ + 2H_2O$

**Equation 2.** $2NO_3^- + 10e^- + 12H^+ \rightarrow N_2 + 6H_2O$

Nitrification is often coupled with denitrification in tidal wetlands because of the spatial variability of oxygenated microsites in the soil. This variability is created in part by the oxygenation of the rhizosphere, favoring nitrification in the top 10-20 mm of the soil (Risgaard-Petersen and Jensen, 1997). Nitrification is an aerobic reaction that oxidizes ammonium ($NH_4^+$) to nitrate, a reactant in denitrification (Equation 2). The oxygenated microsites created by roots and rhizomes have been shown to increase the rate of coupled nitrification and denitrification reactions by a factor of six (Reddy et al. 1989; Risgaard-Petersen and Jensen 1997). The ability of vegetation to create these oxygenated microsites allows them to stimulate the coupling of nitrification and denitrification. Poplar Island marshes are dominated by *S. alterniflora* in the low marsh (Staver et al., 2020). *S. alterniflora* can create oxygenated microsites around its rhizomes through oxygen diffusion from its leaves to its roots and into the surrounding soil. This is made possible by thin, longitudinal vessels found in *S. alterniflora* leaves (Maricle and Lee, 2002). Gases like $O_2$ should be able to travel freely from leaf to roots via this path. The oxygen content

of the plant decreases from the leaves, where photosynthesis occurs, to the roots where there is no photosynthesis, creating a gradient which drives oxygen into the roots of the plant (Teal and Kanwisher, 1965). Another gradient exists within the rhizosphere. Below the top few millimeters of soil, salt marshes are highly reduced and low in oxygen (Schlesinger and Bernhardt, 2012). This gradient from the oxygenated roots to the reduced soil drives the oxygen into the surrounding soil via gaseous diffusion (Teal and Kanwisher, 1965). The extent of this gradient and size of oxygenated microsites are likely affected by the amount of biomass and role of primary production in the marsh.

Another reduction pathway that $NO_3^-$ undergoes in tidal marshes is dissimilatory nitrate reduction to ammonium (DNRA). DNRA is a two-step process that reduces $NO_3^-$ to nitrite ($NO_2^-$) (Equation 3a) then $NO_2^-$ to $NH_4^+$ (Equation 3b). This transformation is performed by obligate anaerobes in anoxic environments, including some wetland sediments, where nitrate availability is low and labile carbon (C) is high (Schlesinger and Bernhardt, 2020). Overall, in coastal wetlands, the importance of DNRA to nitrate reduction varies greatly and is generally less understood than the contribution of denitrification (Giblin et al., 2013). While denitrification removes reactive N from tidal marsh systems as $N_2$ gas, DNRA maintains N in the system as $NH_4^+$. It is important to understand how $NH_4^+$ is produced and maintained within tidal marshes, as it is the preferred form of reactive N for uptake by *S. alterniflora* (Mendelssohn, 1979).

**Equation 3a.** $NO_3^- + 2e^- + 2H^+ \rightarrow NO_2^- + H_2O$

**Equation 3b.** $NO_2^- + 6e^- + 8H^+ \rightarrow NH_4^+ + 2H_2O$

Edaphic algae may influence the variability of tidal marsh denitrification rates. Edaphic algae are primary producers that reside on the surface of tidal marsh soils and have been observed growing in thick mats in the Poplar Island marshes (Staver et al., 2021). These algal

mats are often associated with increased N mineralization and soil stabilization (Lucas et al., 2003; Tobias et al., 2003). The $O_2$ from edaphic algal photosynthesis can create oxygenated areas that promote nitrification. The $NO_3^-$ produced from this process, and labile organic C from edaphic algal biomass decomposition are two important ingredients in denitrification (An and Joye, 2001; Cornwell et al., accepted). The shading effect of macrophytes can limit edaphic algal growth by decreasing the amount of available photosynthetically active radiation (PAR) to the surface of the marsh soil. Increased macrophyte biomass production may impact the edaphic algal community and potentially the N cycling in the soil. Both macrophytes and edaphic algae compete with nitrifying and denitrifying bacteria for reactive N, which can stifle nitrification and denitrification (McGlathery et al., 2007). The impact of edaphic algae on N cycling processes is influenced by the balance of photosynthesis and respiration, as well as nutrient availability (An and Joye, 2001; Risgaard-Petersen et al., 2004).

One characteristic of the marsh soils on Poplar Island is the high concentration of nutrients, especially N. The depletion of oxygen in bottom waters in Chesapeake Bay leads to the accumulation of ammonium in bottom sediments (Kemp et al., 2005). This store in bottom sediment nutrients is enhanced in the navigational channels of Chesapeake Bay, where higher sedimentation rates lead to heightened ammonium accumulation (Cornwell and Owens, 2011). The high ammonium concentration in Poplar Island marsh pore waters may stimulate increased nitrification and therefore denitrification. The denitrification reactions in salt marshes have been suggested to play a significant role in reducing the effects of anthropogenic nutrient loading. It is therefore important to understand the effect of wetland management practices, such as prescribed burns, on these processes.

Previous studies exploring the impact of prescribed burns on nitrogen cycling have focused on forest, grassland, and heathland ecosystems. Zhang et al. (2018) investigated soil mineral N content and the rates of potential nitrification and denitrification one month and three months after a prescribed burn of an Australian suburban forest. They found that potential nitrification rates significantly increased following the burn, likely due to the increase of soil aeration by charcoal deposits following the burn. In this study, denitrification rates initially decreased, then significantly increased three months after the burn due to the increase in soil pH (Zhang et al., 2018). Li and Herbert (2004) reported similar effects of a prescribed burn on nitrification rates in Chinese Wildryegrass grasslands. They found that nitrification rates were initially higher in burned grasslands than unburned grasslands because increased soil temperatures in the burned grasslands drove increased microbial metabolic activity. This pattern was not reflected in the soil nitrate, which significantly increased in burned grasslands later in the growing season, likely due to initial uptake from increased plant growth stimulated by the burn (Li and Herbert, 2004). The effects of prescribed burns on these processes are largely understudied in tidal wetlands, where tidal inundation creates anoxic zones and nitrification reactions are typically coupled with denitrification. This study aims to investigate these effects in the tidal wetlands of Poplar Island.

Fires have been reported to promote species like *S. alterniflora* and *S. patens*, causing a flush of growth in the following growing season (Flores et al., 2011). A study by Bickford et al. (2012) explored the potential mechanisms behind this increase, such as canopy removal and ash deposition, and speculated the importance of earlier and increased access to sunlight by marsh plants. Other potential mechanisms remain unaddressed. The objective of the prescribed burn on Poplar Island was to decrease growth limitation by insect herbivory and pathogens. This increase

in plant growth can affect the spatial variation of oxygenated microsites. Howes and Teal (1994) found that taller, more productive plants had larger aerenchyma, promoting gas transport throughout the plant. This increased gas transport would allow the belowground biomass to oxygenate the sediments around the roots and rhizomes. The relationship between denitrification rates and the impact of marsh burning on belowground plant production remains undocumented (Nyman and Chabreck, 1995). Because of the increase in production and therefore soil oxygenation, as well as the reported increase in nitrification following burns in other systems, I hypothesize that the flush of new growth following the prescribed burn will cause an increase in coupled nitrification and denitrification in the burned marshes compared to the control sites.

This increase in soil oxygenation would also suppress the activity of DNRA microbes; especially without sulfidic conditions, these obligate anaerobes would not thrive (Schlesinger and Bernhardt, 2020). Alternative $NO_3^-$ respiration pathways are less important at lower sulfide concentrations (Murphy et al., 2020). I hypothesize that the importance of DNRA in Poplar's tidal marshes would be low, especially in the burn plots, due to the increase in soil oxygenation brought on by the increase in biomass production.

To address the first hypothesis, burned and unburned control plots were established in three of Poplar Island's tidal marshes. Vegetation surveys and biogeochemical measurements were conducted throughout the growing seasons before and after the burn. Vegetation characteristics like stem height and stem density were monitored throughout both growing seasons to estimate the response of *S. alterniflora* to the prescribed burn. Live aboveground and total belowground plant biomass production was estimated at the end of the 2024 growing season to further characterize the vegetation response. Soil-water exchange of dissolved gases ($N_2$ and $O_2$) and nutrients ($NH_4^+$ and $NO_x^-$) were measured from intact soil core incubations twice per

growing season before and after the burn. These measurements were used to estimate N cycling and edaphic algal photosynthesis rates, as well as soil respiration. Soil chlorophyll-*a* concentrations were measured from subsamples from the cores to estimate edaphic algae production. Concurrently with the sediment-water exchange measurements, soil porewater ammonium and hydrogen sulfide concentrations were measured. This measurement, along with soil temperature, salinity, and water levels were analyzed to investigate potential drivers behind interannual variation in N transformation processes during this study.

To address the second hypothesis, a nitrate addition experiment was conducted in July and October of the growing season following the prescribed burn. The intact sediment cores used to investigate the impact of the prescribed burn on sediment biogeochemistry were spiked with nitrate following the initial incubation. The same measurements were made the following day to investigate the presence of DNRA without the limitation of nitrate availability. This study explores how the increase of tidal marsh plant growth following prescribed burns impacts nitrification-coupled denitrification and identifies the presence of DNRA in Poplar Island's tidal marshes.

## *Materials and Methods*

### Study Site

This study was conducted in the low marsh habitat on Poplar Island. Triplicate treatment (burn) and control plots were established in three marsh sections, called cells, of different ages (Figure 1). A prescribed burn took place on March 18, 2024, in the burn plots of Cells 1A (planting completed in 2009), 1B (2012), 3A (2015). To determine the effect of prescribed burns on nitrogen cycling in the tidal marshes of Poplar Island, soil biogeochemical pools and rate

processes of the soils were examined both before and after the prescribed burn. A complementary survey of plant characteristics and insect populations was developed and helped inform the biogeochemical interpretations.


**Figure 1.** Study site locations on Poplar Island, MD, USA with insets showing the three marsh cells that were burned. Cells are depicted in geographical and chronological order of completion, with the oldest cell, 1A at the top and the youngest cell, 3A at the bottom. The unburned control plots are outlined in green, and the burned plots are outlined in red. Imagery courtesy of US Army Corps of Engineers.

**Vegetation monitoring**

Three sites were established in both the burn and control plots in each of the three marsh cells, for a total of eighteen study sites. Vegetation was monitored bi-monthly from April to October in the growing seasons before and after the prescribed burn (2023 and 2024, respectively). Stem density and stem heights were measured at each of the eighteen sites. Stem density was calculated by counting the number of stems in a 0.1 $m^2$ quadrat and scaled up to 1 $m^2$. Ten stem heights were measured to the nearest centimeter within a meter of each vegetation monitoring site. The prescribed burn did not cover the complete area of the established burn plots (Figure 2) and therefore did not reach all of the original vegetation monitoring sites. In order to capture the effect of the burn, these vegetation monitoring sites were moved into the nearest burned patch.

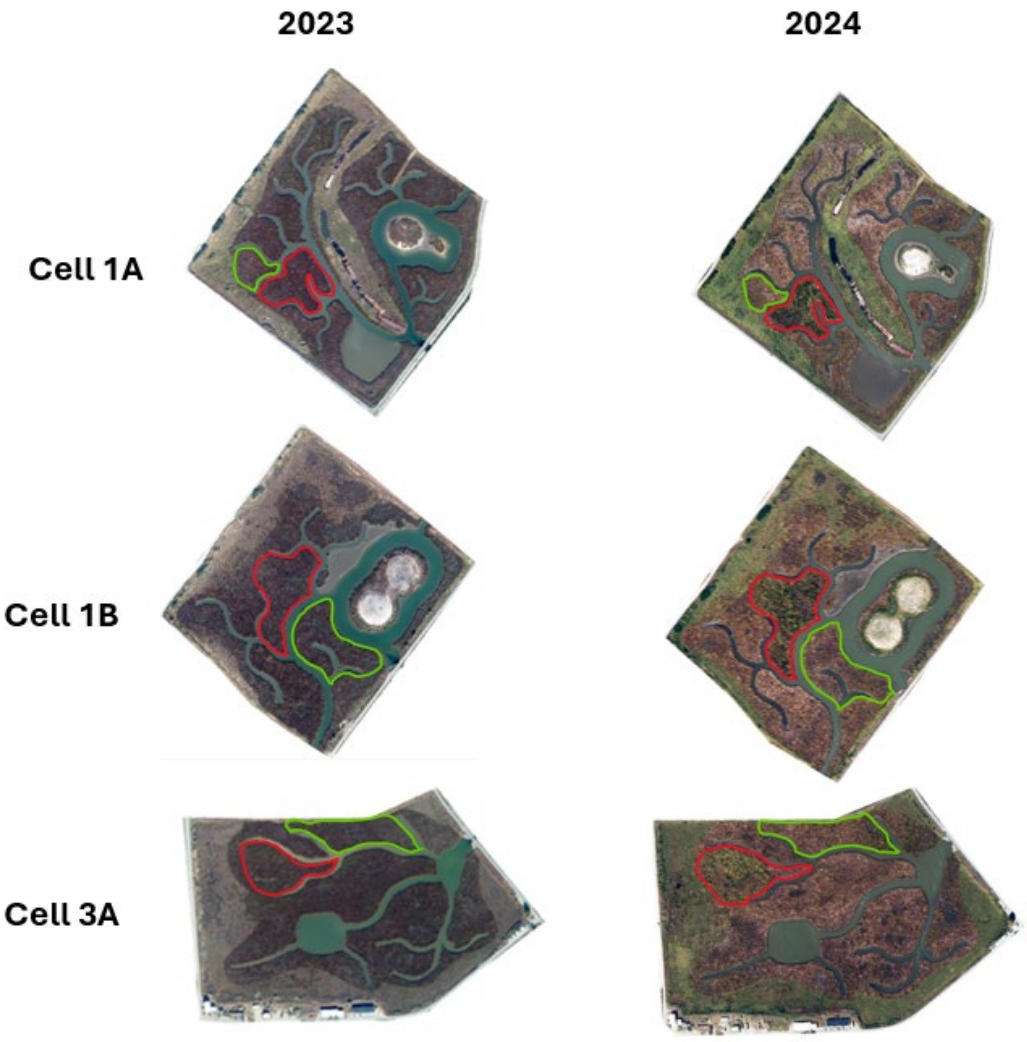


**Figure 2**. Remote sensing imagery from Unite States Army Corps of Engineers (USACE) of the three cells before (2023) and after (2024) the burn. Unburned control plots are outlined in green and burned plots are outlined in red.

**End of season biomass measurements**

Aboveground plant biomass was quantified at the end of the postburn growing season, following methods from Staver et al. (2020). A 0.25 $m^2$ quadrat was randomly placed near all eighteen vegetation monitoring plots in October 2024. All plant biomass within the quadrat was harvested at ground level and brought back to Horn Point Laboratory, where each sample was sorted into live and dead biomass. After drying at 60˚C for three days, the samples were weighed. To measure the accumulated belowground biomass (macro-organic matter, MOM), soil

cores were taken from within the aboveground biomass quadrats at each site using 7.3 cm diameter x 30 cm length piston corers. The length of each soil core was measured before 0.009 M sodium hexametaphosphate was added to soak overnight in a plastic bag. The slurry created was rinsed over a 1 mm sieve to remove sediment from the root and rhizome matter, which was dried at 60 ˚C for three days and weighed.

**Soil core incubations**

In each treatment and control plot, two intact sediment cores were collected, for a total of twelve cores. Cores were collected twice before the burn (July and October 2023) and twice after the burn (July and October 2024). The cores were collected by driving 7 cm diameter acrylic cylinders into the marsh surface to a depth of approximately 15 cm. Extracted cores were capped and transported to Horn Point Laboratory, where they were bubbled overnight in ambient water collected from a tidal creek in Cell 1B. Intact core incubation time courses were carried out with methods from Owens and Cornwell (2016). One core filled with only water was included to correct for water column metabolic activity. Incubations were carried out at the ambient temperature and salinity of the water in this inlet, measured with a YSI 30 Salinity, Conductivity, Temperature probe.

After bubbling overnight with ambient air to fully saturate the water columns with oxygen, sequential dark and light incubation time courses were carried out. Samples were drawn from the water column above each core once every hour for four hours in the dark. After these were collected, a 115V broad spectrum Tek Light system with an irradiance of 225 mmol photons $m^{-2}$ $s^{-1}$ was turned on over the cores to begin the light incubation and stimulate microalgal photosynthesis. Samples were collected over three time intervals of approximately forty-five minutes.

Samples for $N_2$ and $O_2$ analyses were collected into 7 mL stoppered glass vials and preserved with 10 μL of half-saturated mercuric chloride ($HgCl_2$), with a replicate sample collected at the first time point to determine analytical replication. Samples were stored underwater close to the incubation temperature. Ammonium ($NH_4^+$) and nitrate/nitrite ($NO_x^-$) samples were collected into 20 mL syringes, and 5 mL was syringe-filtered (0.4 μm) to two 7 mL centrifuge tubes for $NH_4^+$ and $NO_x^-$, analysis, respectively. Samples were frozen until analysis.

In July and October of 2024, a nitrate addition experiment was performed on the intact sediment cores. Following the first incubation, 250 mL of 0.1M $NaNO_3$ solution was added to each incubation tub and the water reservoir. The cores were left to bubble overnight before overlying water samples were taken for analysis of dissolved gases and nutrients using the same methods from the initial core incubations.

**Soil pore water chemistry**

Pore water chemistry was determined with twelve equilibrators prepared using the methods outlined by Hesslein (1976) and deployed concurrently with sediment core collections at the same sites. Equilibrators contained four 2.5 cm diameter wells covered with a Nucleopore dialysis membrane (0.2 μm), located at depths of 2, 5.25, 8.5, and 12 cm below the surface. Equilibrators were left on site for two weeks. Immediately after retrieval, water from each well was pushed through a 0.45 μm polyether sulfone (PES) filter into a 5 mL vial and frozen until analysis. A solution of N,N-dimethyl-p-phenylenediamine sulfate and ferric chloride in acidic medium was added to a filtered 1 mL sample in the field for colorimetric analysis of $H_2S$ in the laboratory using the methods for determination of sulfide outlined by Parsons et al. (1984).

**Dissolved gas analyses and flux calculations**

Measurement of the flux of dissolved nitrogen gas ($N_2$) and oxygen gas ($O_2$) between the soil core and water column was modified from methods used by Kana et al. (1994). A membrane inlet mass spectrometer (MIMS) was used to measure the ratios of nitrogen to argon gas ($N_2$:Ar) and oxygen to argon gas ($O_2$:Ar) of the water collected in the 7 mL vials. The MIMS instrument consisted of a quadrupole mass spectrometer with a U-shaped tube holding a silicon capillary membrane inlet and stainless-steel capillary tube through which water was pumped to the membrane tube (Kana et al., 1994). Standards of deionized water from a flask immersed in a thermostatic bath were recorded after sets of samples from every two to three cores to calculate the drift of the isotopic signal. $N_2$:Ar and $O_2$:Ar ratios were used along with a given Ar concentration under the measured ambient temperature and salinity to calculate $N_2$ and $O_2$ concentrations of the water column under the assumption that Ar remained constant. This is because while $N_2$ and $O_2$ concentrations are affected by both physical and biological processes, Ar concentrations are influenced by physical processes alone (Kana et al., 1994). Biogeochemical fluxes were calculated based on the rate of analyte change over time, sediment area, and water volume. The fluxes of $N_2$ are expressed on a $N_2$-N basis for comparison to other N fluxes. $O_2$ fluxes were used to estimate soil respiration. $O_2$ fluxes measured in the dark incubation were subtracted from $O_2$ fluxes measured in the light incubation to calculate edaphic algal photosynthesis.

**Colorimetric nutrient analyses and flux calculations**

Solid phase $NH_4^+$ and pore water $NH_4^+$ concentrations were measured using the alternative method for determination of ammonia and pore water $H_2S$ concentrations were measured using the determination of sulfide using methylene blue (Parsons et al 1984). Solid

phase $NO_x^-$ from the soil core incubations was measured via manual vanadium (III) reduction based on procedures from Doane and Horwáth (2003). The samples were colorimetrically analyzed using a Shimadzu UV-VIS Spectrophotometer with an ASC-5 Auto Sample Changer.

**Chlorophyll-*a* measurements**

To investigate the presence of edaphic algae in each plot, a sample was taken from the top centimeter of each core following each incubation and frozen until analysis. Total and active chlorophyll-*a* (chl-*a*) of each sample were measured using methods for fluorometric determination of chlorophylls and phaeopigments adapted from Parsons et al. (1984).

**Potential environmental controls on denitrification**

Surface salinity data from 2023 and 2024 was downloaded from the Chesapeake Bay Program DataHub Water Quality CBC4.1E monitoring station off of Kent Point. Ambient surface salinity measurements were taken from the tidal creek on the east side of Cell 1B on the dates of intact core collections in 2023 and 2024. These four data points were added to the salinity data from the Datahub. Hourly water level data (mean sea level, MSL) was downloaded from the National Oceanographic and Atmospheric Administration's (NOAA) station in Annapolis, MD (Sation ID: 8575512). Soil temperatures from 2023 and 2024 were downloaded from University of Maryland Center for Environmental Science's (UMCES) Poplar Island annual monitoring dataset. Temperatures were logged using Onset HOBO Water Temp Pro v2 loggers.

**Statistical analyses**

To evaluate changes in stem density and average stem height over time and in response to burn treatment, multiple t-tests comparing the change in stem density and the change in stem

height from 2023 to 2024 between the two plot treatments were conducted. False discovery rate correction was applied to adjust p-values for the multiple comparisons by month. Multiple t-tests were also conducted for each month, comparing the average heights between 2023 and 2024. FDR correction was applied to adjust the p-values for multiple testing. One-way analyses of variance (ANOVAs) were conducted to investigate whether the plot treatment (control vs burn) described a significant amount of variability in live aboveground and total belowground plant biomass.

Two-way analyses of variance were conducted to determine whether the time of sampling (2023 vs 2024) and plot treatment described a significant amount of variability in dissolved gas and nutrient fluxes, edaphic algal photosynthesis, and chl-*a* concentration. To determine whether the sampling month influenced differences between growing seasons, two sample t-tests with p-values were conducted using Holm's method to control Type 1 errors. To assess variability by marsh age, one-way ANOVAs were conducted. The direction and strength of the correlation between edaphic algal photosynthesis and chl-*a* concentration was analyzed using Pearson's correlation coefficient. The impact of the nitrate addition on dissolved gas and nutrient fluxes was analyzed using a t-test. Shapiro-Wilk tests and Levene's test were performed on the data and the residuals of the analyses of variance to test normality and homogeneity of variance, respectively. Due to the sample size (see Results section) and the assumption of homogeneity of variance being met (Levene's Test, $p>0.05$), these analyses were robust to non-normality. RStudio 2024.12.0 and R Version 4.4.2 (Base R and packages tidyr, dplyr, purr, and rstatix) were used to run statistical analyses.

*Results*

**Vegetation response**

Average stem height at each vegetation monitoring site increased over the growing season, (April to October) in both years (Figure 3). The average stem heights in 2023 ranged from 12.8 cm in Cell 1A in April to 169.4 cm in Cell 3A in October. In 2024, average stem heights ranged from 21.3 cm in Cell 1B in April to 188.7 cm in Cell 3A in October. Stems were taller in 2024 than in 2023 regardless of plot treatment in April ($p<0.0001$, $t=4.79$, $n=180$), June ($p<0.0001$, $t=8.73$, $n=180$), and August ($p<0.0001$, $t=3.77$, $n=180$), but not in October ($p=0.2$, $t=1.30$, $n=180$). Stems in Cell 3A were taller than stems in Cells 1A and 1B in both 2023 and 2024. Average stem height appears taller in the burn plots than control in Cells 1B and 3A, though this response is not statistically significant for April ($p=0.78$, $t=-0.28$, $n=120$), June ($p=0.16$, $t=1.52$, $n=120$), August ($p=0.08$, $t=1.91$, $n=120$) nor October ($p=0.07$, $t=1.98$, $n=120$).

Stem density at each vegetation monitoring site appeared to stay the same over the growing season in both years (Figure 4). In 2023, stem density ranged from 10 stems/$m^2$ in Cell 3A in April to 680 stems/$m^2$ in Cell 1A in October. Stem density in 2024 ranged from 120 stems/$m^2$ in Cell 1A in August to 790 stems/$m^2$ in Cell 1A in April. Stem density was highly variable and was greater in 2023 than 2024 in April ($p=0.01$, $t=2.66$, $n=18$) and June ($p=0.05$, $t=2.03$, $n=18$), but greater in 2024 than 2023 in August ($p=0.01$, $t=-2.63$, $n=18$). There was no difference between 2023 and 2024 for October stem densities ($p=0.40$, $t=-0.86$, $n=18$). There did not appear to be a difference between plot treatments in April ($p=0.42$, $t=0.83$, $n=18$), June ($p=0.50$, $t=0.70$, $n=18$), and August ($p=0.29$, $t=1.10$, $n=18$).

End of growing season live aboveground plant biomass did not vary significantly between marsh cells, but did respond to plot treatment (Figure 5). Live AG biomass was

significantly greater in burn plots than control plots (p=0.0248, F=12.290, n=18), but did not differ with marsh age (p=0.69, F=0.43, n=18). Mean live AG biomass was 636.4 (± 87.7) g dry weight (gdw)/$m^2$ in the control treatment and 1065.2 (±73.1) gdw/$m^2$ in the burn treatment. Mean BG biomass was 3422.1 (±520.1) gdw/$m^2$ in the control treatment and 4075.2 (±555.6) gdw/$m^2$ in the burn treatment but was not significantly different between treatments (p=0.65, F=0.25, n=18) or marsh age (p=0.13, F=4.39, n=18).

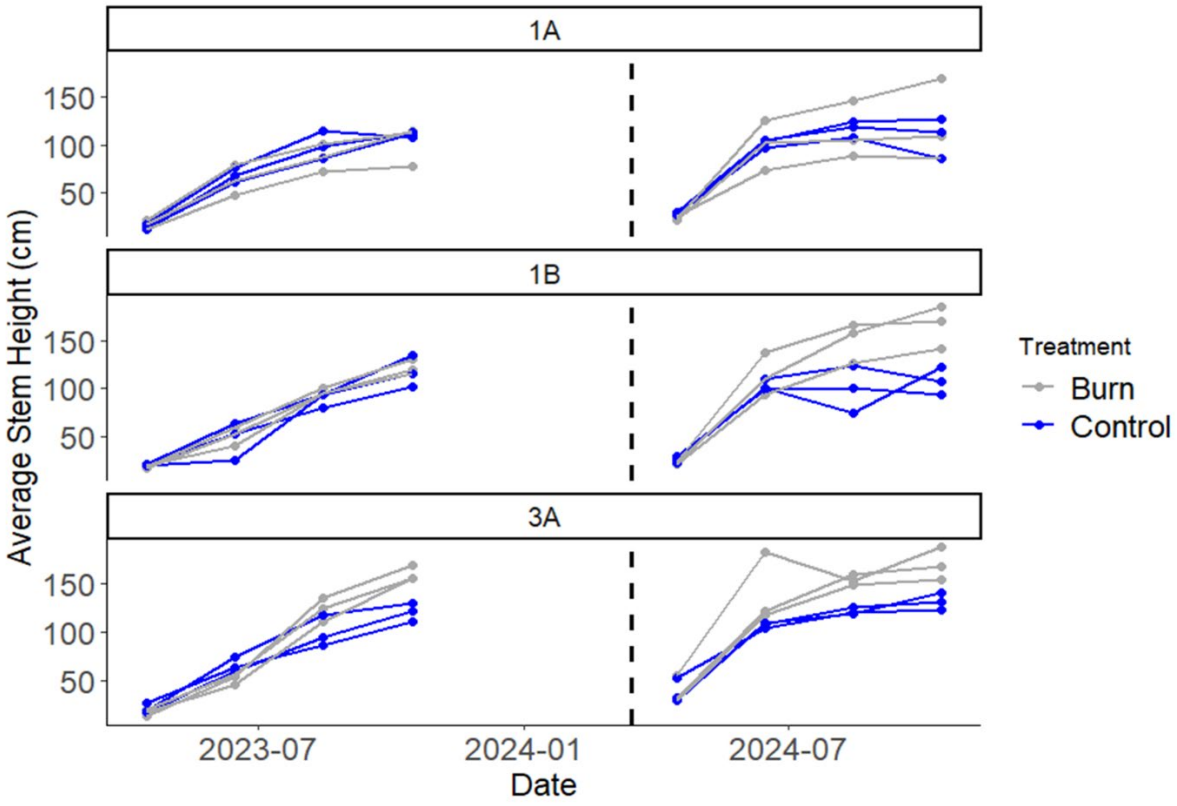


**Figure 3.** The average of ten stem heights of each vegetation monitoring site in the three study cells. Each site is represented by an individual line. Blue represents the control treatment and gray represents the burn treatment. The dashed black line indicates the prescribed burn in March 2024

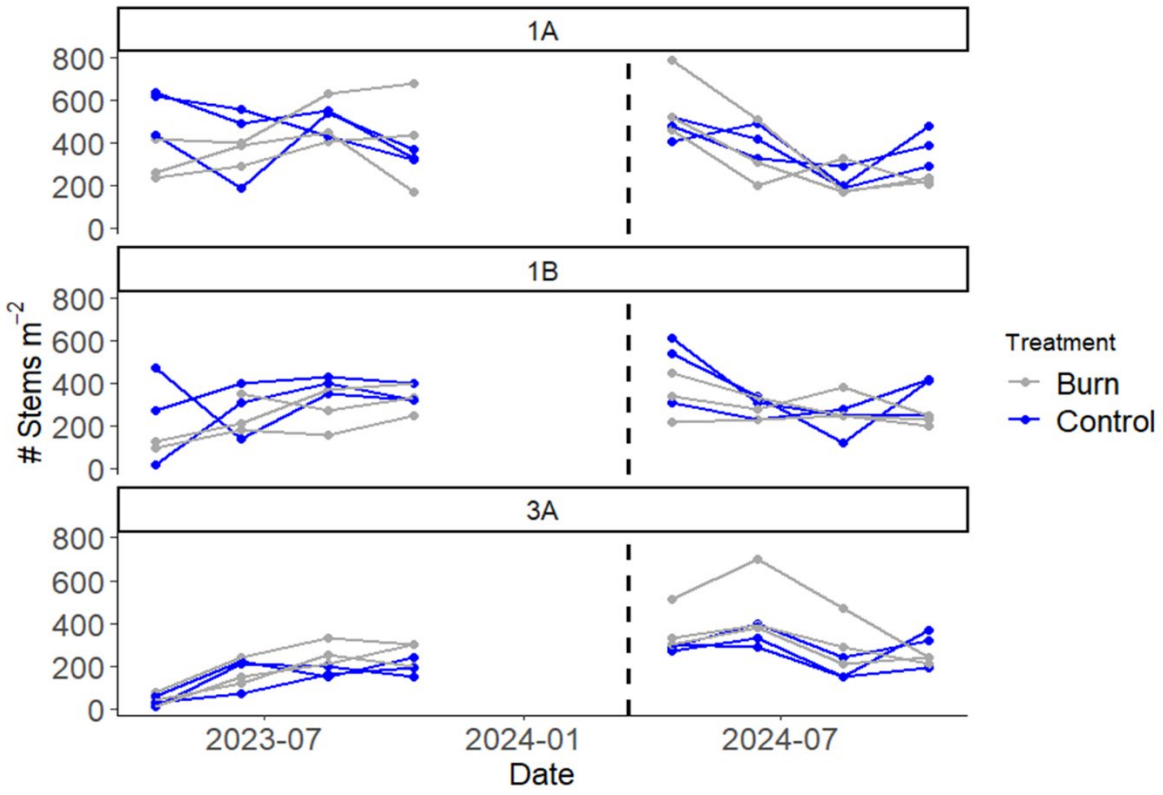


**Figure 4.** Stem density of each vegetation monitoring site in the three study cells represented as number of stems per square meter. Each site is represented by each individual line. Blue represents the control treatment and gray represents the burn treatment. The dashed black line indicates the prescribed burn in March 2024.

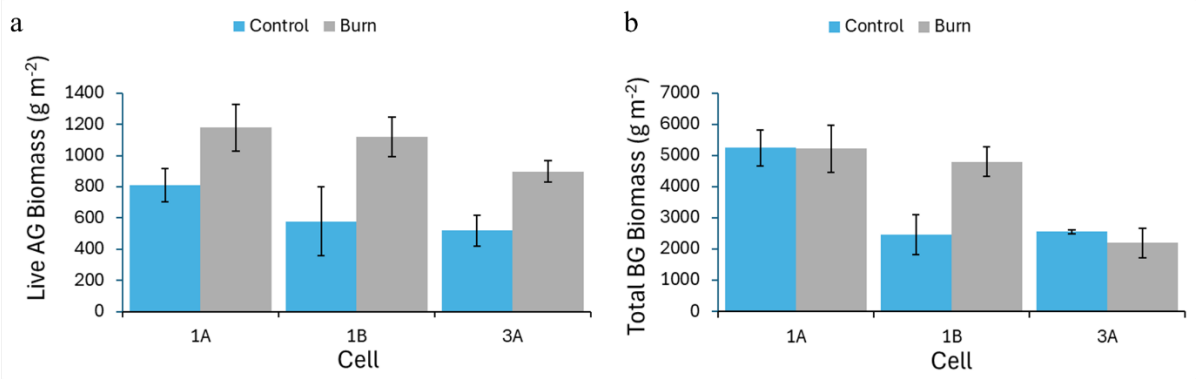


**Figure 5.** Live aboveground plant biomass (a) and total belowground root and rhizome biomass (b). Blue represents control treatment and gray represents burn treatment. Error bars represent standard error.

## Nitrogen fluxes

Dissolved $N_2$-N gas fluxes showed a net efflux from the sediment, with fluxes during the dark incubation (dark fluxes) averaging 257.66 (± 31.80) µmol/m$^2$h in July 2023, 151.05 (±

16.61) μmol/$m^2$h in October 2023, 114.94 (± 25.01) μmol/$m^2$h in July 2024, and 95.51 (± 17.54) μmol/$m^2$h in October 2024 (Figure 6a). Dissolved $N_2$ efflux from the sediment is interpreted as denitrification. The average dark $N_2$-N fluxes were not different between burn and control treatments (p=0.51, F=0.432, n=45) but were significantly different between the two growing seasons. Dark $N_2$-N fluxes were significantly higher in 2023 than in 2024 in both July (p=0.006, t=-3.53, n=24) and October (p=0.05, t=-2.39, n=21).

Dark $NH_4^+$ fluxes showed a net efflux from the sediment in July 2023, which decreased in October 2023 and the 2024 growing season, switching to a net uptake in July 2024 (Figure 7a). Dark $NH_4^+$ fluxes averaged 664.84 (± 78.24) μmol/$m^2$h in July 2023, 46.21 (± 25.26) μmol/$m^2$h in October 2023, -141.87 (± 26.46) μmol/$m^2$h in July 2024, and 16.45 (± 12.52) μmol/$m^2$h in October 2024. No strong difference between the dark $NH_4^+$ fluxes was detected between burn and control treatments (p=0.69, F=26.86, n=48). Dark $NH_4^+$ fluxes were more positive in July 2023 than July 2024 (p<0.0001, t=9.77, n=24) but did not differ between October 2023 and October 2024 (p=0.61, t=1.06, n=24). Dark $NO_x^-$ fluxes showed no significant response to burn treatment (p=0.72, F=0.13, n=44) or growing season (p=0.49, F=0.49, n=44) (Figure 7b). Dark $NO_x^-$ fluxes averaged -80.30 (± 12.74) μmol/$m^2$h in July 2023, -15.53 (± 9.66) μmol/$m^2$h in October 2023, -15.10 (± 26.46) μmol/$m^2$h in July 2024, and -49.58 (± 53.00) μmol/$m^2$h in October 2024.

**Oxygen fluxes**

The oxygen data for both years showed a net uptake, with dark oxygen fluxes averaging -4064.12 (± 391.56) μmol/$m^2$h in July 2023, -2087.39 (± 231.97) μmol/$m^2$h in October 2023, -1735.48 (± 349.32) μmol/$m^2$h in July 2024, and -1791.21 (± 304.16) μmol/$m^2$h in October 2024 (Figure 6b). The average dark oxygen fluxes did not significantly differ between burn and

control treatments ($p<0.0001$, $F=2.43$, $n=45$), but did show interannual variation (Figure 4). Dark oxygen fluxes were significantly greater in July 2023 than in July 2024 ($p=0.0008$, $t=4.44$, $n=24$) and did not differ between October 2023 and October 2024 ($p=0.36$, $t=0.91$, $n=21$). Edaphic algal photosynthesis reflected oxygen efflux from the sediment (Figure 6c). Algal photosynthesis averaged 4050.96 (± 548.63) μmol/$m^2$h in July 2023, 2402.43 (± 310.26) μmol/$m^2$h in October 2023, 3006.74 (± 509.36) μmol/$m^2$h in July 2024, and 1544.10 (± 256.00) μmol/$m^2$h in October 2024. Edaphic algal photosynthesis did not differ between plot treatments ($p=0.07$, $F=3.59$, $n=45$). Edaphic algal photosynthesis did not differ between July 2023 and July 2024 ($p=0.18$, $t=-1.41$, $n=24$) or between October 2023 and October 2024 ($p=0.07$, $t=-2.29$, $n=21$).

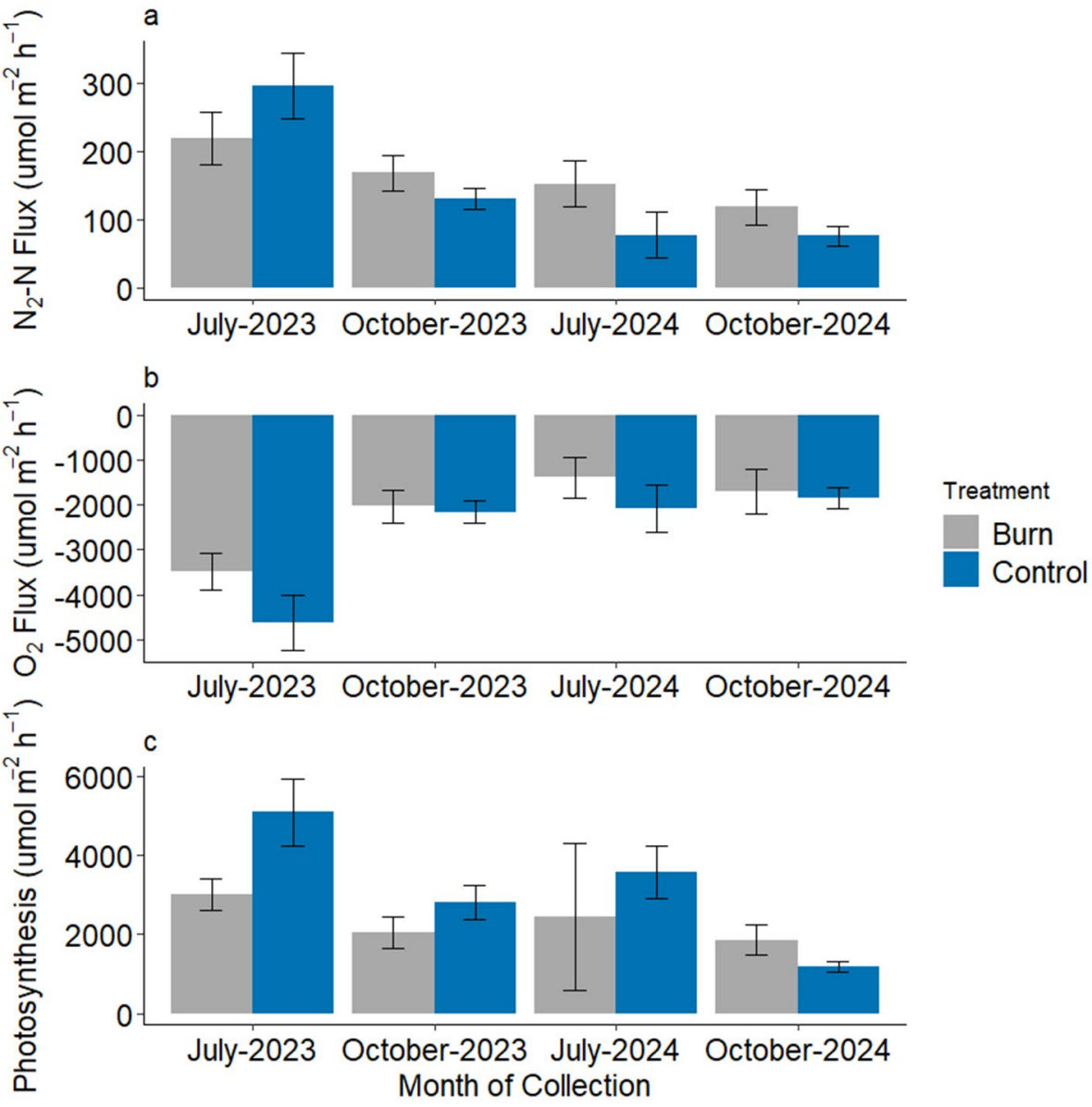


**Figure 6.** Average dark $N_2$-N (a) and $O_2$ (b) fluxes and edaphic algal photosynthetic rate (c). Gray represents burn treatment and blue represents control treatment. Error bars represent standard error. Positive numbers indicate a net release from the soil, while negative numbers indicate net uptake into the soil.

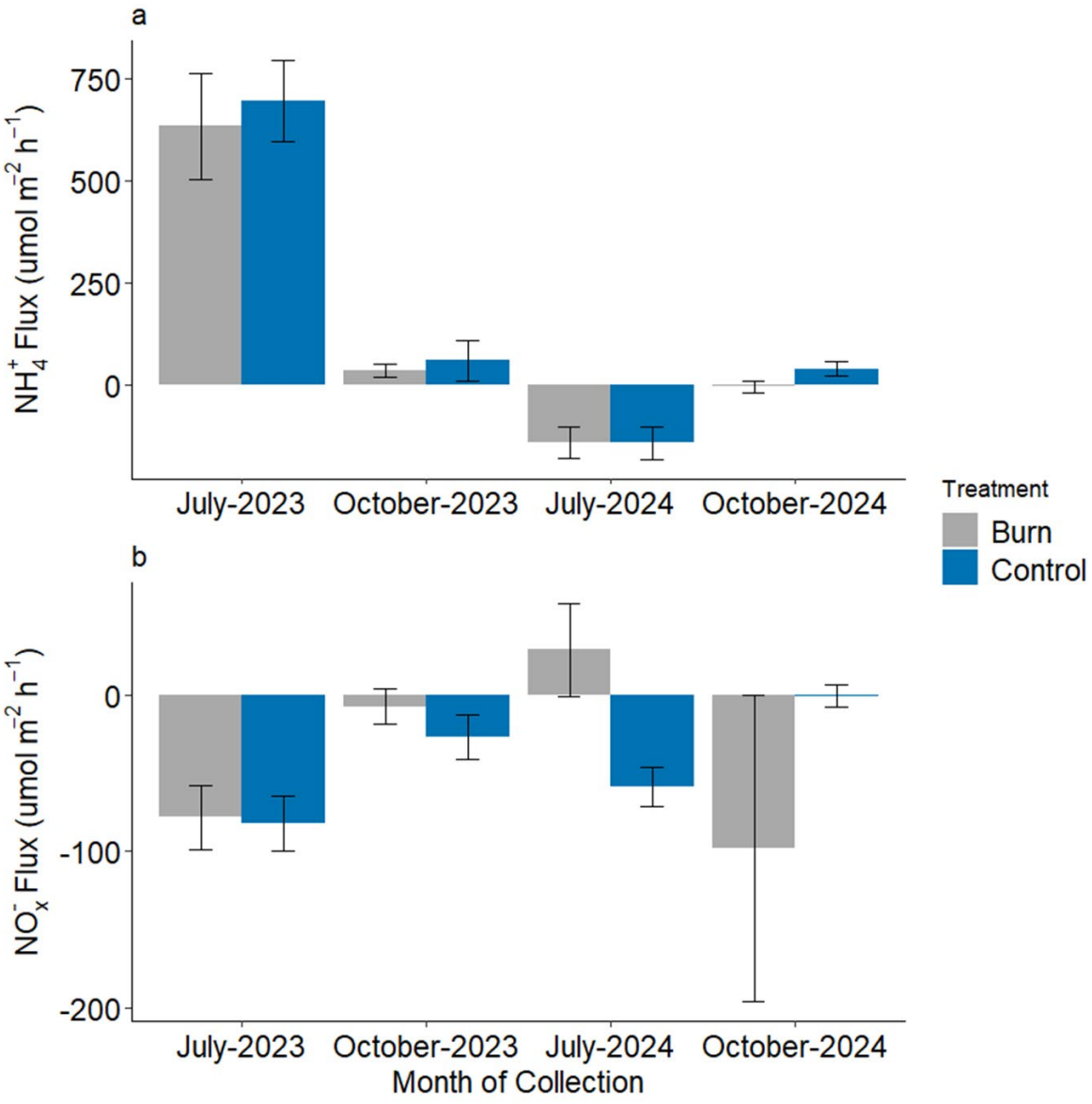


**Figure 7**. Average dark $NH_4^+$ (a) and $NO_x^-$ (b) sediment-water exchange. Gray represents the burn treatment and blue represents the control treatment. Error bars represent standard error. Positive numbers indicate a net release from the soil, while negative numbers indicate net uptake into the soil.

**Soil pore water chemistry**

Across all four sample dates (July 2023, October 2023, July 2024, and October 2024), pore water $NH_4^+$ increased with depth (Figure 8a and b). The concentration of pore water $NH_4^+$ did not significantly differ among the three marsh cells ($p=0.43$, $F=0.779$, $n=188$) nor with plot

treatment (p=0.31, F=1.07, n=188). Pore water $NH_4^+$ was higher in 2024 than in 2023 (p=0.05, F=4.47, n=188).

Hydrogen sulfide ($H_2S$) also increased with depth but exhibited a peak in concentration between five- and nine-centimeters depth (Figure 8c and d). The concentration of pore water $H_2S$ appeared to be greater in the control plots compared to the burn plots in 2024, but this difference was not statistically significant (p=0.35, F=0.93, n=188). Pore water $H_2S$ appeared greater in July 2024 than in July 2023, though this difference was also not statistically significant (p=0.08, F=3.31, n=188).

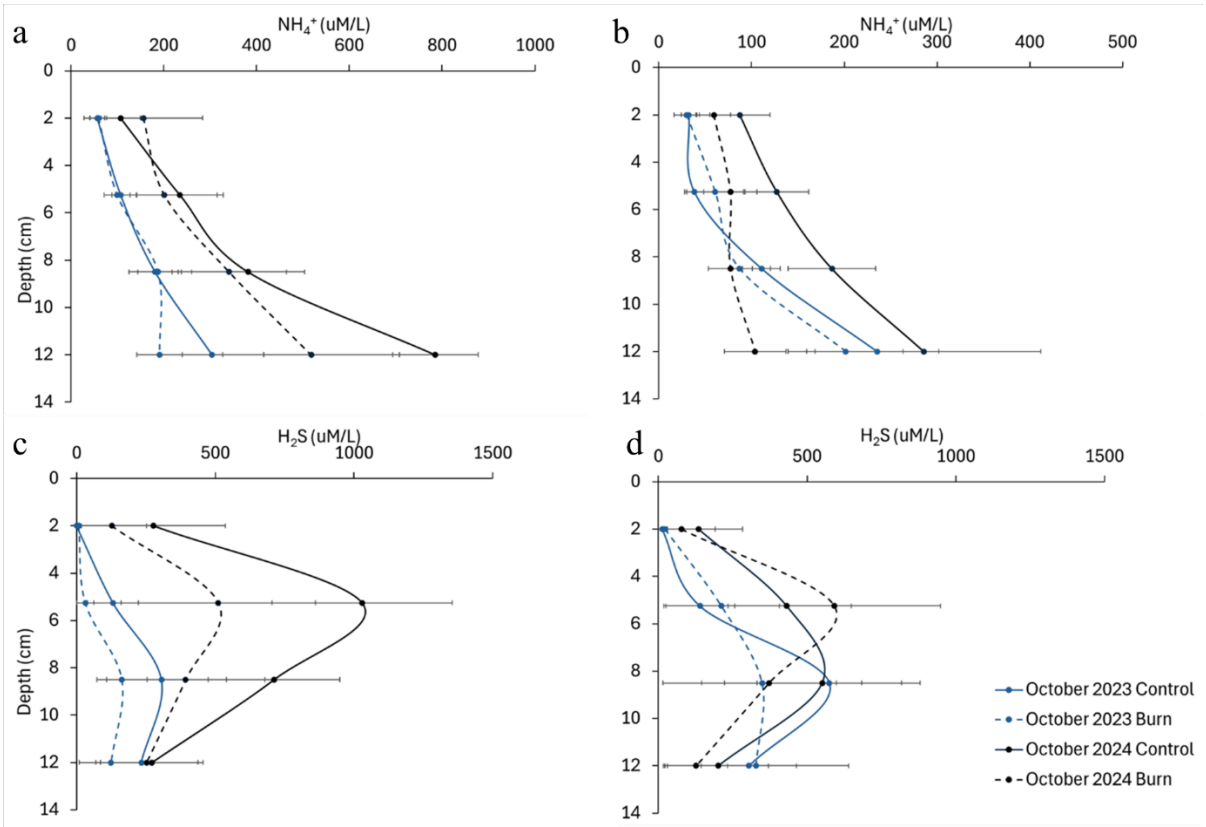


**Figure 8.** Average pore water profiles of $NH_4^+$ in July (a) and October (b) and $H_2S$ in July (c) and October (d) in the top 12 cm of marsh sediment measured concurrently with intact core dissolved gas and nutrient flux measurements. Blue lines represent pore water profiles from 2023, and black lines represent profiles from 2024. Solid lines represent control plots and dashed lines represent burn plots. Error bars indicate standard error.

**Chlorophyll-*a***

Chlorophyll-*a* concentrations with correction for phaeopigments represent the standing crop of edaphic algae due to its correlation with gross algal productivity (Gallagher, 1971). Chl-*a* did not strongly differ over time nor between the three marsh cells in this study (Figure 9). It was, however, greater in the control plots than the burn plots throughout the growing season following the prescribed burn ($p=0.0229$, $F=16.23$, $n=24$). Mean active chl-*a* was 42.38 (± 7.95) mg/m$^2$ in control plots and 163.54 (± 58.07) mg/m$^2$ in burn plots in 2024. Chlorophyll-*a* appeared to be weakly positively correlated with rates of edaphic algal photosynthesis ($R = 0.39$, $p=0.008$, $t=2.78$, $n=48$).

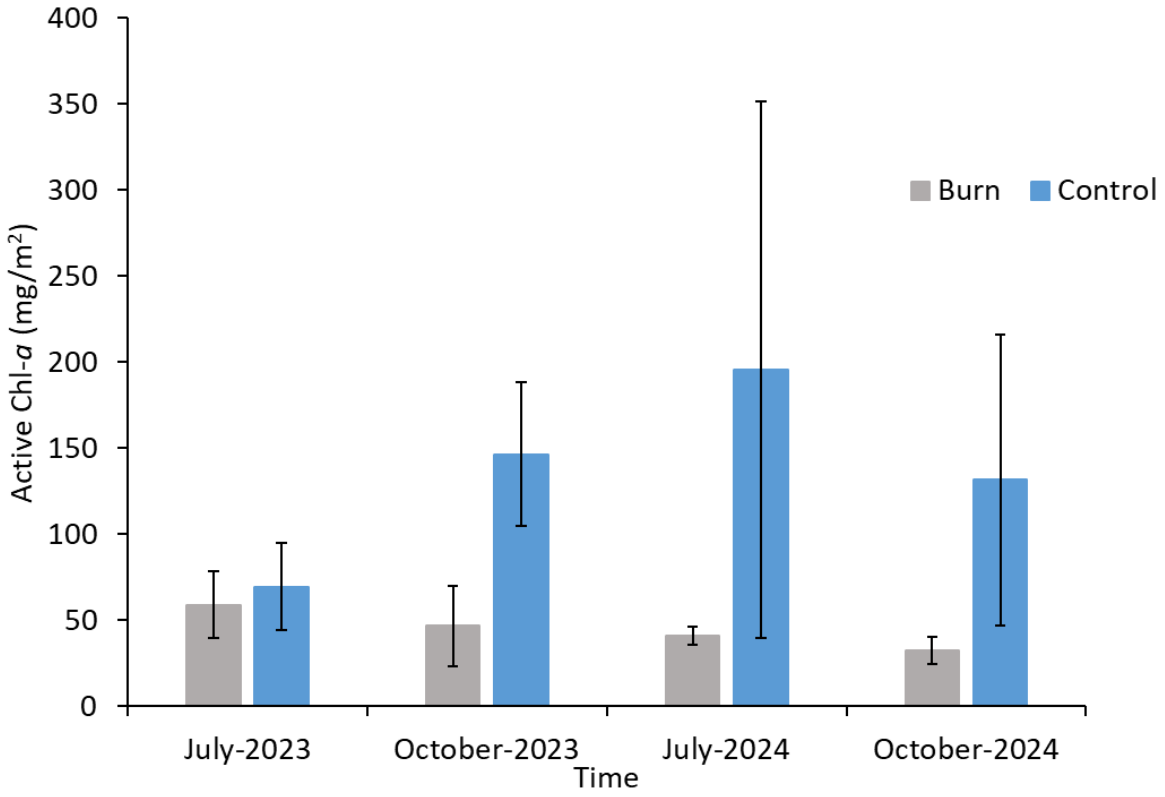


**Figure 9**. Active chlorophyll-*a* content of the top centimeter from the intact sediment cores used in sediment-water exchange incubations. Blue bars represent active chl-*a* in the control plots and the gray bars represent active chl-*a* in the burn plots. Error bars represent standard error.

**Potential environmental controls on denitrification**

The water level from the Annapolis monitoring station was significantly higher in 2024 than in 2023 ($p<0.0001$, $t=-9.46$, $n=10272$) throughout the entire year (Figure 10a). The average water level was 0.262 (± 0.002) m above MSL in 2023 and 0.297 (± 0.003) m above MSL in 2024. There did not appear to be a significant difference in water level in July or October of either year, however.

Salinity increased over the growing season from May to October in both 2023 and 2024 (Figure 10b). The salinity was significantly higher in 2023 than in 2024 ($p=0.008$, $t=3.681$, $n=7$). The average salinity was 11.36 (± 0.91) ppt in 2023 and 7.39 (± 0.58) ppt in 2024. The salinity of the tidal inlet in Cell 1B was 13.49 ppt and 16.45 ppt in July and October of 2023, respectively; and 9.4 ppt and 14.7 ppt in July and October of 2024, respectively.

The soil temperatures of June and July were stable during the month preceding the July core incubations in both 2023 and 2024 (Figure 10c). The average soil temperature was lower in July 2023 than in July 2024 ($p<0.0001$, $t=-6.98$, $n=1488$).

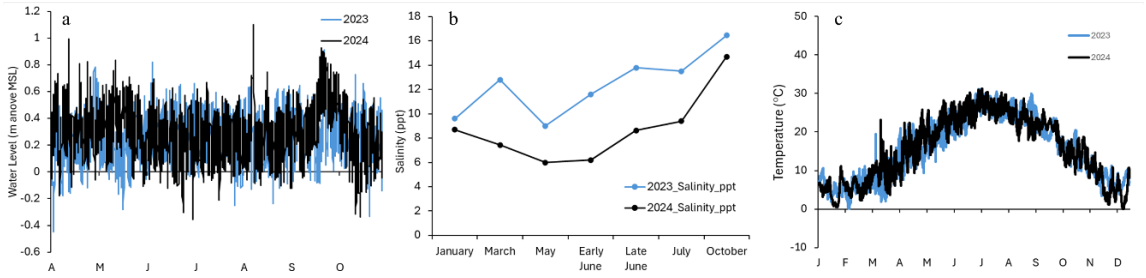


**Figure 10.** Potential environmental controls on denitrification. Hourly water level data (a) from the growing seasons of 2023 and 2024 are downloaded from the National Oceanographic and Atmospheric Administration's (NOAA) station in Annapolis, MD. Salinity data (b) from January to June of 2023 and 2024 downloaded from Chesapeake Bay Program DataHub Water Quality CBC4.1E monitoring station off Kent Point and salinity data from July and October of 2023 and 2024 measured from Poplar Island Cell 1B tidal inlet. Soil temperature from 2023 and 2024 (c) measured from Poplar Island Cell 1C.

**Soil-water exchange under nitrate enrichment**

There did not appear to be a response of the mean dark $N_2$-N flux to the prescribed burn following $NO_3^-$ addition ($p=0.83$, $t=-0.84$, $n=22$). The average dark $N_2$-N efflux from the

sediment was greater during the nitrate addition incubation period than the control incubation period during both July ($p=0.007$, $t=3.74$, $n=24$) and October ($p=0.001$, $t=4.89$, $n=19$). The average dark $N_2$-N production was 2.5 times greater following $NO_3^-$ addition in July (Figure 11a) and 2.1 times greater following $NO_3^-$ addition in October (Figure 11d). The average dark $NH_4^+$ flux was greater during the $NO_3^-$ addition incubation than the control incubation in July ($p=0.01$, $t=3.71$, $n=22$), but showed no response to $NO_3^-$ addition in October ($p=0.89$, $t=-0.13$, $n=22$) (Figure 12a and b). In July, the average dark $NH_4^+$ flux began as a net uptake in the incubation before $NO_3^-$ addition and became net release from the soil following $NO_3^-$ addition. There did not appear to be a response to the prescribed burn during either of the $NO_3^-$ addition incubations in regard to average dark $NH_4^+$ (0.92, $t=0.10$, $n=22$).

The mean dark oxygen flux did not differ between the burn and control treatments during either of the $NO_3^-$ addition incubations ($p=0.83$, $t=0.56$, $n=22$) nor between cells ($p=0.31$, $F=1.26$, $n=22$). The mean dark $O_2$ uptake was greater following $NO_3^-$ addition in July ($p=0.05$, $t=-2.06$, $n=24$), but did not differ between the two incubations in October ($p=0.99$, $t=0.96$, $n=19$) (Figure 11b and e). In July, the average dark $O_2$ uptake was about 1.7 times greater following $NO_3^-$ addition. Edaphic algal photosynthesis did not change in response to $NO_3^-$ addition in either July ($p=0.99$, $t=-0.03$, $n=24$) (Figure 10c) and October ($p=0.99$, $t=-1.00$, $n=19$) (Figure 11c and f). There did not appear to be a difference in this response between the burn and control cores ($p=0.52$, $t=-1.45$, $n=22$).

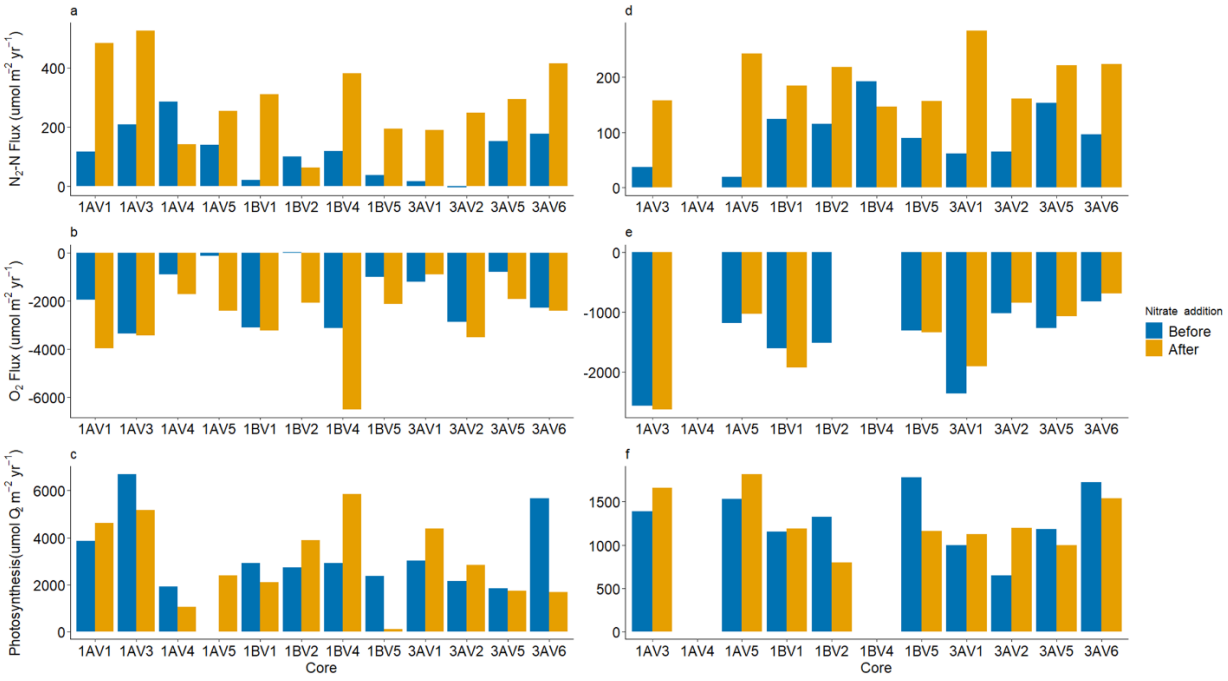


**Figure 11.** Average dark $N_2$-N fluxes in July (a) and October (d), $O_2$ fluxes in July (b) and October (e), and algal photosynthetic rate in July (c) and October (f) before and after nitrate addition. Blue represents fluxes calculated from the incubation before the nitrate addition and gold represents fluxes calculated from the incubation after the nitrate addition.

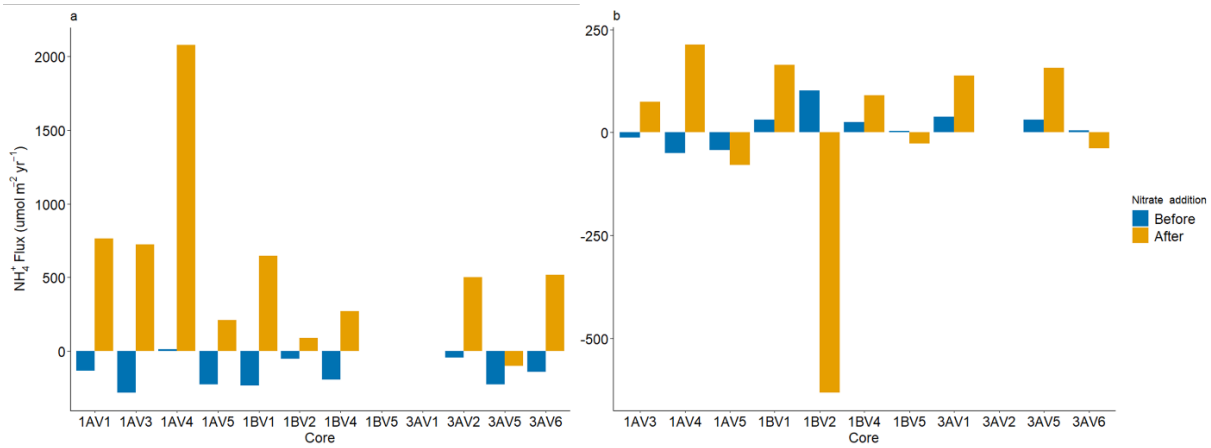


**Figure 12.** Average dark $NH_4^+$ fluxes in July (a) and October (b) before and after nitrate addition. Blue represents fluxes calculated from the incubation before the nitrate addition and gold represents fluxes calculated from the incubation after the nitrate addition.

## *Discussion*

### Vegetation response

The prescribed burn appeared to stimulate increased aboveground plant production, but not belowground. Stem density showed no response to the burn. Previous studies also did not

find a significant response in *Spartina spp.* stem density to prescribed burning of tidal marshes in Blackwater National Wildlife Refuge in Cambridge, MD (Blackwater) (Leonard et al., 2010; Bickford et al., 2012). However, one study in Blackwater's tidal marshes did find an increase in *S. alterniflora* stem density in response to prescribed burning (Flores et al., 2011). Stem height appeared to be greater in the burn plots of Cells 1B and 3A. These cells are the younger two of the three marshes. It is possible that not all of vegetation monitoring sites were moved to burned areas and that the burn effect was not adequately captured in all plots.

At the end of the 2024 growing season, the biomass harvest indicated 1.7 times more live aboveground biomass in the burn plots than the control plots. This number represents new biomass production from only the 2024 growing season, as any standing dead biomass from previous growing seasons was sorted out. These findings agree with the findings of previous studies on prescribed burning in tidal marshes (Leonard et al., 2010; Flores et al., 2011; Bickford et al., 2012). The increase in aboveground live biomass in the burn plots supports the hypothesis that prescribed burning stimulates increased plant production.

Total belowground biomass did not differ between burn and control plots in October 2024. These findings also agree with previous studies, which have indicated no significant response of belowground biomass production to burns (Leonard et al., 2010). Though we took three replicate cores in each plot, our small sample size may not have captured the burn effect on belowground biomass due to the heterogeneity of the marsh. It is also important to note that our belowground biomass measurements included both live and dead belowground biomass and did not represent only new production from the 2024 growing season. Belowground biomass productivity is influenced by a number of factors like marsh elevation, salinity, and nutrient availability (Kirwan and Guntenspergen, 2012; Alldred et al., 2017). Some of these factors are

independent from the prescribed burn and may have played a larger role in belowground biomass production than the response of the plants to the burn.

**Dissolved gas and nutrient fluxes**

Average dark $N_2$-N fluxes agreed with past denitrification measurements of mesohaline tidal wetlands around Chesapeake Bay, with the exception of the $N_2$-N fluxes from July 2023 (Merrill 1999; Boynton et al., 2008). These fluxes were similar other measurements from Poplar Island marshes (Cornwell et al., 2022). Average dark $N_2$-N fluxes in July 2023 were almost double some of these measurements.

There did not appear to be any significant change in soil nitrogen dynamics in response to the prescribed burn. The sediment-water exchange of dissolved $N_2$ and $O_2$ gases, as well as nutrients like $NH_4^+$ and $NO_x^-$ did not differ significantly between burn and control sites. The hypothesis that prescribed burning stimulates increased nitrification-coupled denitrification is not supported. Though replicates were measured in this study, the number of core incubations required to cover a large area of the marsh is unrealistic, and the effect of the burn may not have been captured due to heterogeneity in the marsh. Moreover, because live plants were not included in these cores, these observations may not have captured the oxygenation of the rhizosphere. Cores were taken as close to plants as possible and many included root materials. Additionally biogeochemical measurements were made in the middle and at the end of the two growing seasons, so any impacts of the burn on these N cycling processes at the beginning of the growing season were not recorded. This suggests then that the effect of the prescribed burn may have been on a small temporal scale and therefore did not influence long-term N dynamics in the marsh.

Though there was no variation in soil-water exchange in response to the burn, interannual variation was evident, especially between July 2023 and July 2024. Various potential environmental controls such as temperature, salinity, and water level can impact denitrification rates. Prior studies have found a decrease in tidal wetland nitrification and denitrification at higher salinities (Osborne et al., 2015). However, the salinity throughout 2023 was greater than in 2024, while nitrogen fixation was unchanged, indicating that salinity did not drive changes in nitrogen fixation. This result aligned with other studies that found no significant link between estuary salinity and N transformation rates, likely because tidal marsh soil microbes are adapted to small fluctuations in salinity (Hu et al., 2021). Kim et al. (2023) have observed microbial communities that were likely less specialized in the tidal marshes of Poplar Island. This may suggest that microbial communities on Poplar Island are resilient to changes in salinity.

Soil temperature on Poplar Island was higher in 2024 than in 2023, while N cycling rates decreased between 2023 and 2024. This does not agree with prior studies that have found an increase in microbial metabolic rates in response to higher temperatures (Kaplan et al., 1979; Bowes et al., 2022). However, some studies on the response of tidal marsh denitrifiers to temperature have also observed a temperature selection for distinct populations of denitrifiers (Kaplan et al., 1977). Because of this, different populations of denitrifiers may dominate during different temperature regimes, complicating the response of microbial denitrification to differences in temperature.

Inundation frequency and duration can drive variability in tidal marsh soil oxygenation, which can influence biogeochemical cycling (Schlesinger and Bernhardt, 2020). Mean annual water levels were higher in 2024 than in 2023 overall, though it is important to note that in the 30 days immediately before each intact core collection, this difference was not observed. In other

tidal marsh systems, increased denitrification rates have been observed in response to more frequent tidal inundation (Bai et al., 2017; Hu et al., 2019). While higher water levels do increase tidal inundation frequency, our study sites are already in lower elevation marshes and may not experience a drastic change in inundation frequency under higher water levels. Because of this, higher water levels may increase the amount of time our sites are flooded. Longer periods of tidal inundation are associated with anoxic conditions, resulting in increased pore water sulfide concentrations in *S. alterniflora* dominated tidal marshes (Alldred et al., 2020). This is reflected in the higher pore water sulfide concentrations in July 2024 than in July 2023. These higher concentrations likely suggest more reduced conditions, possibly due to the increased water levels throughout early 2024. The pore water measurements were constrained to the top 12 cm of the soil, capturing only the conditions in the root zone. For this reason, concentrations from all four depths were averaged together for comparison. High sulfide concentrations inhibit nitrification and can promote DNRA over complete denitrification in estuarine sediments (Joye et al., 2016; Murphy et al., 2020). Lower nitrification rates would lower $NO_3^-$ production and therefore denitrification rates, which we observed in July 2024. It is also possible that lower sulfide concentrations in 2023 signify decreased sulfate reducers and therefore a removal of limitation by competition with sulfate reducing bacteria for resources on denitrifier communities. This may partially explain the increase in N cycling processes.

Pore water $NH_4^+$concentrations were also measured for both 2023 and 2024 and the lower concentration in 2023 persisted for both July and October. Lower pore water $NH_4^+$ coupled with increased N transformation rates may be a sign of increased microbial uptake. Another potential cause for this difference in $NH_4^+$ concentration is plant uptake of pore water nutrients. While *S. alterniflora* takes up both forms of reactive N analyzed in this study, $NH_4^+$ is

preferentially taken up due to the increased residence time of $NH_4^+$ in marsh soils (Mendelssohn, 1979; Mozdzer et al., 2011). However, other factors like salinity may influence the rate of uptake by plants. Higher salinity inhibits $NH_4^+$ uptake by *S. alterniflora* (Bradley and Morris, 1991). Salinity of ambient waters was higher in 2023. Marsh plants compete with soil microbes for $NH_4^+$, so lower rates of plant uptake in 2023 would allow increased access to $NH_4^+$ for nitrifiers and result in increased rates of N cycling. Another potential environmental control on denitrification rates is the water column concentration of nutrients like $NO_3^-$, which was not explored in this study. Water column $NO_3^-$ loading can lead to increased denitrification (Koop-Jakobsen and Giblin, 2010). Further work investigating controls on interannual variation of tidal marsh N cycling is required to understand the increase in N cycling processes observed in 2023 and should include measurements of ambient nutrient concentrations.

**Presence of edaphic algae**

The presence of edaphic algae has been connected to the establishment of nitrification and denitrification in the tidal marshes of Poplar Island (Cornwell et al., accepted). It is therefore important to understand the impact management strategies like prescribed burns have on the presence and productivity of edaphic algae. Neither measured rates of edaphic algal photosynthesis or biomass measured from active chl-*a* exhibited interannual variation. However, chl-*a* concentration decreased in response to the prescribed burn. The increase in aboveground biomass production by *S. alterniflora* may have reduced the photosynthetically active radiation (PAR) reaching edaphic algae as the growing season progressed. Another potential explanation is that the increased macrophyte production may have also decreased available reactive N for edaphic algal uptake. Edaphic algal photosynthesis did not exhibit a response to the burn. This difference in response to the prescribed burn is not surprising. While there is a positive

relationship between photosynthetic rate and chl-*a* concentration, as we observed in this study, photosynthetic rate is controlled by multiple other factors like light, nutrient availability, and temperature (Laws et al., 2016). The lack of response in edaphic algal photosynthetic rate to the burn may also partially explain some of the lack of response in the dissolved nutrient and gas fluxes as well. Despite decreased edaphic algal production suggested by the decrease in chl-*a* concentration, oxygenation by photosynthesis did not change. Edaphic algal photosynthesis can stimulate nitrification-coupled denitrification via soil oxygenation (An and Joye, 2001). It is unlikely then that nitrification would increase without an increase in oxygenation from edaphic algae or macrophytes. It is possible that we did not capture a response to the burn due to the small sample size in proportion to the marsh, despite the replication in this study, due to heterogeneity in the marsh. To further investigate the impact of the prescribed burn on the edaphic algal community and the relationship of this response to the response of biogeochemical processes, cores could be selected for edaphic algal presence and compared to bare cores. To measure the shading effect of increased plant growth following the burn, measurements of light received by the edaphic algae in the field could be stimulated in laboratory incubations of soil cores containing edaphic algae.

**Nitrate addition experiment**

The $NO_3^-$ addition experiments in 2024 were intended to remove the limitation by $NO_3^-$ availability in an effort to investigate the potential for DNRA in Poplar Island's tidal marshes. The cores from our burn study incubations were used to capture any effects the burn may have had on this potential. There was no difference in the changes in soil-water exchange of dissolved gases and nutrients in response to the nitrate addition between cores collected in the burn and

control plots. This suggests that the burn did not impact the present N cycling pathways present at each site.

Both $NH_4^+$ and $N_2$ production have been used as indicators of DNRA and denitrification, respectively, in other work (Cornwell and Owens, 2011; Fang et al., 2022). The initial intact core incubation revealed a net $NH_4^+$ uptake in July 2024, which became a net efflux following the $NO_3^-$ addition. This and the $N_2$ efflux following $NO_3^-$ addition were similar to the effluxes measured in July 2023. The increase in both measured fluxes suggested an increase in both processes in response to the $NO_3^-$ addition. Both DNRA and denitrification have been shown to increase in response to increased $NO_3^-$ concentration in tidal marshes (Koop-Jakobsen et al., 2010; Li et al., 2019). These results suggest that when the pressure of competition for nutrients is lifted, Poplar Island's tidal marshes have the potential for DNRA. While it is unlikely that Poplar Island's marshes experience ambient nitrate concentrations to the degree of our experiment, some nitrate limitation may be lifted in early spring when snowmelt and precipitation increases nitrate transportation to the bay. Other nutrient-enriched tidal marshes in New England experience DNRA rates that are just as important as denitrification (Koop-Jakobsen and Giblin, 2010). Several environmental factors like salinity, $NO_3^-$ availability, and organic matter availability control the importance of DNRA (Li et al., 2019; Fang et al., 2022). It is important to understand the balance between N removal and recycling processes in this system, as vegetation on Poplar Island depends on N recycling as an important nutrient source (Staver et al., 2021). While we were able to identify the presence of this $NO_3^-$ reduction pathway in soil cores collected from Poplar Island, these are not true rates of DNRA. Further work is necessary to fully elucidate the importance of DNRA in this system.

*Conclusion*

Prescribed burning is a useful management technique that can improve plant health and growth. Based on our results, prescribed burn had the intended effect of promoting plant production. This study tested whether the prescribed burn would also increase nitrogen removal via denitrification. The methods used in this study may not have captured the full rhizosphere effect, as no live plants were included in core incubations. Future work may incorporate live plants into such measurements. However, while the prescribed burn did not result in the expected positive effect of increasing denitrification, the results of this study suggest that there was also no unintended harm to the marsh's biogeochemical cycling either. Strong interannual variation observed in this study may be due to differences in pore water chemistry between the two growing seasons. Future work investigating interannual variation may require longer-term measurements of denitrification over several growing seasons. Elucidation of drivers behind this interannual variation may be possible through laboratory soil core incubations with manipulation of variables like salinity, temperature, and ambient nutrient concentrations.

# Bibliography


Alldred, Mary, Anne Liberti, and Stephen B. Baines. "Impact of salinity and nutrients on salt marsh stability." *Ecosphere* 8.11 (2017): e02010.

Alldred, M., Borrelli, J. J., Hoellein, T., Bruesewitz, D., & Zarnoch, C. (2020). Marsh Plants Enhance Coastal Marsh Resilience by Changing Sediment Oxygen and Sulfide Concentrations in an Urban, Eutrophic Estuary. *Estuaries and Coasts*, *43*(4), 801–813.

An, S., & Joye, S. B. (2001). Enhancement of coupled nitrification-denitrification by benthic photosynthesis in shallow estuarine sediments. *Limnology and oceanography*, *46*(1), 62-74.

Bai, J., Wang, X., Jia, J., Zhang, G., Wang, Y., & Zhang, S. (2017). Denitrification of soil nitrogen in coastal and inland salt marshes with different flooding frequencies. *Physics and Chemistry of the Earth, Parts A/B/C*, *97*, 31-36.

Barbier, E. B., Hacker, S. D., Kennedy, C., Koch, E. W., Stier, A. C., & Silliman, B. R. (2011). The value of estuarine and coastal ecosystem services. *Ecological monographs, 81(2),* 169-193.

Bickford, W. A., Needelman, B. A., Weil, R. R., & Baldwin, A. H. (2012). Vegetation response to prescribed fire in mid-Atlantic brackish marshes. *Estuaries and coasts*, *35*, 1432-1442.

Bowes, K. M., White, J. R., Maiti, K., & Meselhe, E. (2022). Surface water temperature impacts on coastal wetland denitrification: Implications for river reconnection. *Science of the Total Environment*, *828*, 154397.

Boynton, W. R., Hagy, J. D., Cornwell, J. C., Kemp, W. M., Greene, S. M., Owens, M. S., Baker, J.E., & Larsen, R. K. (2008). Nutrient budgets and management actions in the Patuxent River estuary, Maryland. *Estuaries and Coasts*, *31*, 623-651.

Bradley, P. M., & Morris, J. T. (1991). The influence of salinity on the kinetics of $NH_4^+$ uptake in *Spartina alterniflora*. *Oceologia*, *85*, 375-380.

Chesapeake Bay Program. (n.d.). *Wetlands*. Chesapeake Bay Program. https://www.chesapeakebay.net/issues/whats-at-risk/wetlands#:~:text=Shrub%20wetlands%2C%20known%20as%20bogs,runoff%20and%20weakening%20storm%20surges.

Cornwell, J. C., & Owens, M. S. (2011). Quantifying sediment nitrogen releases associated with estuarine dredging. *Aquatic geochemistry, 17*, 499-517.

Cornwell, J. C., Owens, M. S., Staver, L. W., & Stevenson, J. C. (2020). Tidal marsh restoration at Poplar Island I: transformation of estuarine sediments into marsh soils. *Wetlands*, *40*, 1673-1686.

Cornwell, J. C., Owens, M. S., & Staver, L. W. (2022). Nutrient retention and release in eroding Chesapeake Bay tidal wetlands. *JAWRA Journal of the American Water Resources Association*, *58*(6), 940-957.

Cornwell, J. C., Owens, M. S., Staver, L. W., & Stevenson, J. C. (accepted). Tidal marsh restoration at Poplar Island III: establishment of denitrification in a wetland constructed from dredged materials.

Doane, T. A., & Horwáth, W. R. (2003). Spectrophotometric determination of nitrate with a single reagent. *Analytical letters*, *36*(12), 2713-2722.

Fang, X., Yang, Z., & Han, J. (2022). The relative dominance of denitrification and dissimilatory nitrate reduction to ammonium (DNRA) under four vegetation types in a typical coastal wetland. *Applied Soil Ecology*, *177*, 104528.

Fisher, T. R., Hagy, J. I. D., Boynton, W. R., & Williams, M. R. (2006). Cultural eutrophication in the Choptank and Patuxent estuaries of Chesapeake Bay. *Limnology and Oceanography*, *51*(1part2), 435-447.

Flores, C., Bounds, D. L., & Ruby, D. E. (2011). Does prescribed fire benefit wetland vegetation?. *Wetlands*, *31*, 35-44.

Gallagher, J. L. (1971). *Algal productivity and some aspects of the ecological physiology of the edaphic communities of Canary Creek tidal marsh*. University of Delaware.

Giblin, A. E., Tobias, C. R., Song, B., Weston, N., Banta, G. T., & Rivera-MonroyV.H. (2013). The importance of dissimilatory nitrate reduction to ammonium (DNRA) in the nitrogen cycle of coastal ecosystems. *Oceanography*, *26*(3), 124-131.

Hesslein, R. H. (1976). An in situ sampler for close interval pore water studies 1. *Limnology and oceanography*, *21*(6), 912-914.

Howes, B. L., & Teal, J. M. (1994). Oxygen loss from Spartina alterniflora and its relationship to salt marsh oxygen balance. *Oecologia*, *97*, 431-438.

Hu, M., Peñuelas, J., Sardans, J., Huang, J., Xu, K., & Tong, C. (2021). Denitrification rates in tidal marsh soils: The roles of soil texture, salinity and nitrogen enrichment. *European Journal of Soil Science*, *72*(1), 474-479.

Hu, W., Zhang, W., Zhang, L., Lin, X., Tong, C., Lai, D. Y., Chen, Y., & Zeng, C. (2019). Short-term changes in simulated inundation frequency differentially affect inorganic nitrogen, nitrification, and denitrification in estuarine marshes. *Ecological Indicators*, *107*, 105571.

Joye, S. B., & Hollibaugh, J. T. (1995). Influence of sulfide inhibition of nitrification on nitrogen regeneration in sediments. *Science*, *270*(5236), 623-625.

Kana, T. M., Darkangelo, C., Hunt, M. D., Oldham, J. B., Bennett, G. E., & Cornwell, J. C. (1994). Membrane inlet mass spectrometer for rapid high-precision determination of $N_2$, $O_2$, and Ar in environmental water samples. *Analytical chemistry*, *66*(23), 4166-4170.

Kaplan, W. A., Teal, J. M., & Valiela, I. (1977). Denitrification in salt marsh sediments: Evidence for seasonal temperature selection among populations of denitrifiers. *Microbial Ecology*, *3*(3), 193-204.

Kemp, W. M., Boynton, W. R., Adolf, J. E., Boesch, D. F., Boicourt, W. C., Brush, G., Cornwell, J.C., Fisher, T.R., Glibert, P.M.,Hagy, J.D., Harding, L.W., Houde, E.D., Kimmel, D.G., Miller, W.D., Newell, R.I.E., Roman, M.R., Smith, E.M., & Stevenson, J. C. (2005). Eutrophication of Chesapeake Bay: historical trends and ecological interactions. *Marine ecology progress series*, *303*, 1-29.

Kim, C., Staver, L. W., Chen, X., Bulseco, A., Cornwell, J. C., & Malkin, S. Y. (2023). Microbial community succession along a chronosequence in constructed salt marsh soils. *Microbial ecology*, *85*(3), 931-950.

Kirwan, M. L., & Guntenspergen, G. R. (2012). Feedbacks between inundation, root production, and shoot growth in a rapidly submerging brackish marsh. *Journal of Ecology*, *100*(3), 764-770.

Koop-Jakobsen, K., & Giblin, A. E. (2010). The effect of increased nitrate loading on nitrate reduction via denitrification and DNRA in salt marsh sediments. *Limnology and Oceanography*, *55*(2), 789-802.

Leonard, C. A., Ahn, C., & Birch, D. (2010). Above-and below-ground vegetative responses to prescribed fire regimes in a Chesapeake Bay tidal brackish marsh. *Journal of Ecology and Environment*, *33*(4), 351-361.

Laws, E. A., Bidigare, R. R., & Karl, D. M. (2016). Enigmatic relationship between chlorophyll a concentrations and photosynthetic rates at Station ALOHA. *Heliyon*, *2*(9).

Li, Y., & Herbert, S. J. (2004). Influence of prescribed burning on nitrogen mineralization and nitrification in grassland. *Communications in soil science and plant analysis*, *35*(3-4), 571-581.

Li, X., Gao, D., Hou, L., & Liu, M. (2019). Soil substrates rather than gene abundance dominate DNRA capacity in the *Spartina alterniflora* ecotones of estuarine and intertidal wetlands. *Plant and Soil*, *436*, 123-140.

Lucas, C. H., Widdows, J., & Wall, L. (2003). Relating spatial and temporal variability in sediment chlorophyll a and carbohydrate distribution with erodibility of a tidal flat. *Estuaries*, *26*, 885-893.

Maricle, B. R., & Lee, R. W. (2002). Aerenchyma development and oxygen transport in the estuarine cordgrasses *Spartina alterniflora* and *S. anglica*. *Aquatic botany, 74(2),* 109-120.4

Marschner, P. 2012. *Marschner's Mineral Nutrition of Higher Plants.* Academic Press, London.

McGlathery, K. J., Sundbäck, K., & Anderson, I. C. (2007). Eutrophication in shallow coastal bays and lagoons: the role of plants in the coastal filter. *Marine Ecology Progress Series*, *348*, 1-18.

Mendelssohn, I. A. (1979). The influence of nitrogen level, form, and application method on the growth response of *Spartina alterniflora* in North Carolina. *Estuaries*, *2*(2), 106-112.

Merrill, J. Z. (1999). *Tidal freshwater marshes as nutrient sinks: particulate nutrient burial and denitrification* (Doctoral dissertation, University of Maryland, College Park).

Mozdzer, T. J., Kirwan, M., McGlathery, K. J., & Zieman, J. C. (2011). Nitrogen uptake by the shoots of smooth cordgrass *Spartina alterniflora*. *Marine Ecology Progress Series*, *433*, 43-52.

Murphy, A. E., Bulseco, A. N., Ackerman, R., Vineis, J. H., & Bowen, J. L. (2020). Sulphide addition favours respiratory ammonification (DNRA) over complete denitrification and alters the active microbial community in salt marsh sediments. *Environmental Microbiology*, *22*(6), 2124-2139.

Nyman, J. A., & Chabreck, R. H. (1995). Fire in coastal marshes: history and recent concerns. In *Fire in wetlands: a management perspective. Proceedings of the Tall Timbers Fire Ecology Conference* (Vol. 19).

Osborne, R. I., Bernot, M. J., & Findlay, S. E. (2015). Changes in nitrogen cycling processes along a salinity gradient in tidal wetlands of the Hudson River, New York, USA. *Wetlands*, *35*, 323-334.

Owens, M. S., & Cornwell, J. C. (2016). The benthic exchange of $O_2$, $N_2$ and dissolved nutrients using small core incubations. *Journal of Visualized Experiments (JoVE)*, (114), e54098.

Parsons, T.R., Maita, Y., and Lalli, C.M. (1984) A manual of chemical and biological methods for seawater analysis. Oxford, UK, Pergamon, Press, 173pp. DOI : http://dx.doi.org/10.25607/OBP-1830

Petersen, N. R., & Jensen, K. (1997). Nitrification and denitrification in the rhizosphere of the aquatic macrophyte *Lobelia dortmanna L*. *Limnology and Oceanography*, *42*(3), 529-537.

Reddy, K. R., Patrick Jr, W. H., & Lindau, C. W. (1989). Nitrification-denitrification at the plant root-sediment interface in wetlands. *Limnology and oceanography*, *34*(6), 1004-1013.

Risgaard-Petersen, N., Nicolaisen, M. H., Revsbech, N. P., & Lomstein, B. A. (2004). Competition between ammonia-oxidizing bacteria and benthic microalgae. *Applied and environmental microbiology*, *70*(9), 5528-5537.

Schlesinger, W. H., & Bernhardt, E. S. (2020). *Biogeochemistry: an analysis of global change.* Fourth edition. Academic Press.

Sobek, E. A., & Munkvold, G. P. (1999). European corn borer (Lepidoptera: Pyralidae) larvae as vectors of *Fusarium moniliforme*, causing kernel rot and symptomless infection of maize kernels. *Journal of economic entomology, 92(3)*, 503-509.

Staver, L. W., Stevenson, J. C., Cornwell, J. C., Nidzieko, N. J., Staver, K. W., Owens, M. S., Logan, L., Kim, C., & Malkin, S. Y. (2020). Tidal marsh restoration at Poplar Island: II. Elevation trends, vegetation development, and carbon dynamics. *Wetlands*, *40*, 1687-1701.

Staver, L. W., Cornwell, J. C., Nidzieko, N. J., Staver, K. W., Stevenson, J. C., Owens, M., Boynton, W., & Lopez-Gonzalez, L. (2021). The fate of nitrogen in dredged material used for tidal marsh restoration. *Journal of Marine Science and Engineering*, *9*(8), 849.

Staver, L. W., Cornwell, J. C., Nardin, W., Pain, A., Chen, X., Owens, M., (in preparation). *Paul S. Sarbanes Ecosystem Restoration Project at Poplar Island Wetland Cells Monitoring Program: 2024-2025 Studies to Address Sustainability in the Poplar Island Marshes Final Report*. University of Maryland Center for Environmental Science Horn Point Laboratory.

Teal, J. M., & Kanwisher, J. W. (1966). Gas transport in the marsh grass, Spartina alterniflora. *Journal of Experimental Botany*, *17*(2), 355-361.

Tobias, C., Giblin, A., McClelland, J., Tucker, J., & Peterson, B. (2003). Sediment DIN fluxes and preferential recycling of benthic microalgal nitrogen in a shallow macrotidal estuary. *Marine Ecology Progress Series*, *257*, 25-36.

Verhoeven, J. T., Arheimer, B., Yin, C., & Hefting, M. M. (2006). Regional and global concerns over wetlands and water quality. *Trends in ecology & evolution*, *21*(2), 96-103.

Zhang, M., Wang, W., Wang, D., Heenan, M., & Xu, Z. (2018). Short-term responses of soil nitrogen mineralization, nitrification and denitrification to prescribed burning in a suburban forest ecosystem of subtropical Australia. *Science of the total environment*, *642*, 879-886.